


 Cite this: *RSC Adv.*, 2023, **13**, 8025

 Received 9th January 2023  
 Accepted 2nd March 2023

 DOI: 10.1039/d3ra00169e  
[rsc.li/rsc-advances](http://rsc.li/rsc-advances)

## Hydrothiolation of alkynes with thiol–catechol derivatives catalysed by CuNPs/TiO<sub>2</sub>: exploring the reaction mechanism by DFT calculations†

Matías Capurso, Gabriel Radivoy, Fabiana Nador and Viviana Dorn \*

Density functional theory (DFT) calculations were applied to describe the hydrothiolation reaction of activated alkynes with thiols bearing a catechol group. The thiol–yne click (TYC) process was efficiently catalysed by a CuNPs/TiO<sub>2</sub> nanocatalyst giving the corresponding *anti*-Markovnikov vinyl sulphides with high Z-stereoselectivity. Based on the experimental results and DFT studies, a plausible reaction mechanism is proposed, which implies the activation of the carbon–carbon triple bond by coordination to the copper centre, followed by a stereoselective (external) nucleophilic attack to give preferentially the Z-vinyl sulphide isomer. Additionally, experimental and theoretical studies strongly correlate with the proposed synergistic role for the TiO<sub>2</sub> support in the catalytic process.

### Introduction

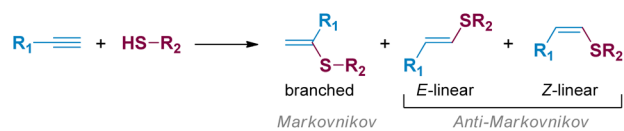
Thiol–yne click (TYC) reaction represents a simple and attractive approach to produce valuable synthetic intermediates such as vinyl sulphides, starting from readily available thiols and alkynes.<sup>1,2</sup> This reaction is commonly promoted by the presence of free radicals,<sup>3</sup> strong acids,<sup>4</sup> bases<sup>5</sup> or transition metals.<sup>6</sup> Through these methodologies, branched and/or linear vinyl sulphides have been obtained in a Markovnikov or *anti*-Markovnikov fashion, respectively (Scheme 1).<sup>7,8</sup>

Furthermore, due to the wide range of applications of these valuable derivatives in the field of materials science, an increasing interest has been focused on new synthetic methodologies for the synthesis of catechol-based molecules under smooth conditions, in a straightforward and atom-efficient way. Novel bioinspired functional materials based on catechol structures have been employed in the preparation of adhesives,<sup>9</sup> capsules,<sup>10</sup> coatings<sup>11</sup> and in the formation of coordination polymer nanoparticles (CNPs),<sup>12</sup> among others. Accordingly, in a recent paper published by our group,<sup>13</sup> we described the TYC reaction between activated alkynes with adjacent electron-withdrawing groups, and thiols bearing catechols pre-synthesized through a versatile Michael addition methodology.<sup>14</sup> The reaction was promoted by a heterogeneous and low-cost metal nanocatalyst composed of copper nanoparticles supported on TiO<sub>2</sub> (CuNPs/TiO<sub>2</sub>), in 1,2-dichloroethane (1,2-

DCE) as the solvent, under heating at 80 °C and in the absence of any added base. Through this novel methodology, thirteen new catechol-bearing vinyl sulphides were obtained, with conversions ranging from good to excellent. Moreover, the reaction was highly regio- and stereoselective towards the *anti*-Markovnikov Z-vinyl sulphide in most of the cases studied.

In terms of the possible mechanisms involved in the metal catalysed hydrothiolation of alkynes, two pathways have generally been proposed; a carbon–carbon triple bond activation followed by the nucleophilic attack of the thiol or an initial activation of the thiol followed by the insertion of the alkyne into the metal–sulphur bond. In this sense, two excellent review articles by Castarlenas, Oro *et al.*,<sup>2</sup> and Beletskaya and Ananikov,<sup>15</sup> highlighted the most important mechanistic aspects regarding the use of transition metal-based catalytic systems for the regio- and stereoselective control of this transformation.

It is known that copper catalysts are able to activate the acetylenic triple bond towards a nucleophilic attack by metal  $\pi$ -coordination. On this matter, Zhang *et al.* reported the CuI-catalysed stereoselective hydrothiolation of alkynes, in the presence of K<sub>2</sub>CO<sub>3</sub> as base, under CO<sub>2</sub> atmosphere and water as proton donor, working in DMSO as the solvent.<sup>16</sup> The authors proposed the carboxylation of the terminal Csp atom promoted by copper-activation of the acetylenic group, and the formation of a cyclic alkene/carboxylate copper complex intermediate as



Scheme 1 Schematic representation of alkyne hydrothiolation.

*Instituto de Química del Sur (INQUISUR-CONICET), Depto. de Química, Universidad Nacional del Sur, Av. Alem 1253, B8000CPB Bahía Blanca, Argentina. E-mail: vdorn@uns.edu.ar*

† Electronic supplementary information (ESI) available: Computational procedure, xyz coordinates and total energies in atomic units for all of the calculated structures. See DOI: <https://doi.org/10.1039/d3ra00169e>



the essential pathway for the observed stereoselectivity towards the *Z*-vinyl sulphides. Beletskaya and coworkers,<sup>17</sup> reported the regio- and stereoselective formation of the corresponding *Z*-( $\beta$ )-alkenyl sulphides starting from alkyl and aryl thiols and terminal alkynes in the presence of CuI and NEt<sub>3</sub> as base. The authors suggested that CuI could activate the carbon–carbon triple bond by acting as a Lewis acid, also favouring the *Z* to *E* isomerisation of the vinyl sulphides, either in protic solvents or after prolonged heating. In another work, Kodomari *et al.*<sup>18</sup> reported that the addition of thiols to methyl propionate was notably accelerated by the presence of neutral alumina (Al<sub>2</sub>O<sub>3</sub>) to give the *Z*-isomer with high stereoselectivity. The authors suggested that alumina basic sites were responsible for the increase in thiol nucleophilicity, while the acid sites were proposed to be activating the carbon–carbon triple bond through coordination with the carboxymethyl group.

In line with these experimental observations and mechanistic proposals by other authors, in our recent work about the TYC reaction catalysed by CuNPs/TiO<sub>2</sub>,<sup>13</sup> we observed that the nature of the support had a strong influence on the stereoselectivity of the reaction. We then speculated with a non-innocent role of the TiO<sub>2</sub> support, that could be synergistically participating in the activation of the alkyne, the thiol or both. Additionally, we proposed that the TiO<sub>2</sub> support could be acting as a fixer for the catechol moiety.<sup>19</sup> In this regard, Terranova,<sup>20a</sup> and also Diebold and coworkers,<sup>20b</sup> computationally evaluated the interaction of one or both of the pyrocatechol hydroxyl groups with different rutile (TiO<sub>2</sub>) faces, by means of DFT methods. In agreement with the experimental data, they observed that in some cases the most stable mode of interaction was a monodentate one, while a bidentate coordination was favoured in other cases, suggesting that both coordination structures could easily interconvert.

From the above, it seems clear that the selectivity of the metal-catalysed hydrothiolation reaction could be influenced by many factors, not only by the nature of the metal catalyst but also by the structure of the starting alkyne, the use of additives, the reaction temperature and/or the solvent. In this scenario, performing theoretical studies regarding the possible intermediates and transition states involved in the reaction mechanism, could shed light on further rational designing of more selective catalytic systems.

In this regard, computational studies about the mechanism involved in metal-catalysed alkyne hydrothiolation are scarce, and only few papers can be found in the scientific literature. Zhang and Wang,<sup>21</sup> have computationally studied the regiochemistry of the Au(i)/NHC-catalysed hydrothiolation of phenylacetylene with thiophenol. By using DFT methods, the authors proposed an alkyne insertion into the metal–sulphur bond as the rate-determining step, the Au(i)/NHC-catalyst showing a superior *anti*-Markovnikov selectivity when compared to Ag(i) and Cu(i) catalysts. More recently, Ananikov *et al.*<sup>22</sup> reported the regioselective hydrothiolation of cyclopropyl acetylenes employing a Pd/NHC complex as precatalyst, in the presence of a base (NEt<sub>3</sub>), a radical trap ( $\gamma$ -terpinene) and toluene as the solvent, giving the corresponding Markovnikov vinyl sulphides. The authors also carried out an in-depth

mechanistic study, by means of both experimental work and computational modelling, focused on the alkyne insertion into the palladium–sulphur bond aiming to disclose, the factors controlling the high regioselectivity observed. Regarding computational modelling studies on the alkyne hydrothiolation reaction promoted by heterogeneous metal-catalysts, Kalluraya and Turukarabettu informed about the hydrothiolation of two heteroaryl acetylenic ketones with 5-phenyl-1,3,4-oxadiazole-2-thiol catalysed by AuNPs/TiO<sub>2</sub> in ethanol, yielding the corresponding *Z*-vinyl sulphides *via* an *anti*-addition process.<sup>23</sup> By means of plane waves DFT methods, together with charges and OM interactions analyses, the authors proposed a reaction mechanism with a first step involving alkyne–gold coordination, a subsequent nucleophilic attack by the thiol at the  $\beta$ -carbon, and final protonation. It is worthy of note that no reaction coordinate was proposed, and both the thiol activation and the role of the metal support were not discussed.

In order to contribute to the rational design of more selective and active catalysts, it is crucial to have an in-depth understanding of the mechanistic aspects involved in each catalytic process. To this end, and inspired by our permanent interest in the use of computational methods for unveiling the main mechanistic aspects of organic transformations,<sup>24</sup> specially those promoted by supported metal nanocatalysts,<sup>25</sup> we present herein a computational theoretical study, based on DFT methods, to shed light on the high stereoselectivity observed in the hydrothiolation of activated alkynes with thiols bearing a catechol group catalysed by CuNPs/TiO<sub>2</sub>.

## Computational methodology

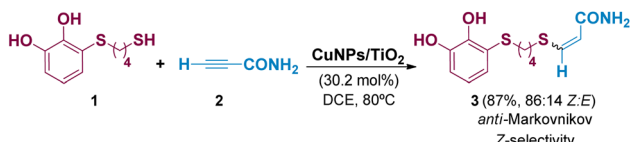
The computational study was performed by using the ORCA software package.<sup>26</sup> The density functional theory (DFT)<sup>27</sup> energies were obtained with the PBE0 functional,<sup>28</sup> applying the D3BJ Grimme's dispersion correction,<sup>29</sup> which is known to be an appropriate methodology for similar mechanistic studies on alkyne hydrothiolation reactions<sup>22</sup> as well as for the modelling of copper complexes,<sup>30</sup> and the triple- $\zeta$  def2-TZVP basis set<sup>31</sup> for all atoms. The energies in solution were obtained with the conductor-like polarizable continuum model (CPCM)<sup>32</sup> using dichloromethane (DCM) as provided by the library of solvents of ORCA v. 4.2.1.

## Results and discussion

As we reported in our previous work,<sup>13</sup> the TYC reaction between a series of thiols bearing a catechol group (1) and different activated alkynes with adjacent electron-withdrawing groups (2) catalysed by CuNPs/TiO<sub>2</sub>, led to the corresponding *anti*-Markovnikov vinyl sulphides (3) with high stereoselectivity towards the *Z*-isomer in most of the cases studied. The reaction conditions are summarised in Scheme 2, showing the reaction between 3-[(4-mercaptopbutyl)thio]benzene-1,2-diol (1) and propiolamide (2) as model starting compounds.

Although the exact mechanism involved for this reaction was difficult to ascertain, based on our previously reported results<sup>25</sup> and those by other groups in the same area, and with the aid of





**Scheme 2** Reaction conditions for the synthesis of vinyl sulphides from activated alkynes and thiols bearing a catechol group.

some additional experiments, the formation of copper acetylides as reaction intermediates (deuterated-vinyl sulphide product was obtained when starting from 3-deuterio-*propiolamide*) and the participation of radical species (hydrothiolation was also efficient in the presence of TEMPO) could be disregarded.

It is worthy of note that the nature of the catalyst support proved to be essential for the hydrothiolation to take place efficiently, and consequently, it needs to be considered in any mechanistic proposal. As above mentioned, Lewis acidic ( $\text{Ti}^{4+}$ ) and/or Lewis basic ( $\text{O}^{2-}$ ) sites on the catalyst support could be acting as a fixer for the catechol moiety through coordination with the catechol hydroxyl groups (a and b in Fig. 1), while the basic sites could be also activating the thiol group (c in Fig. 1).

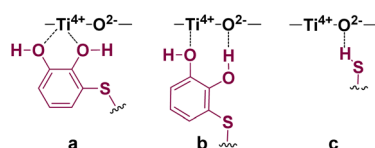
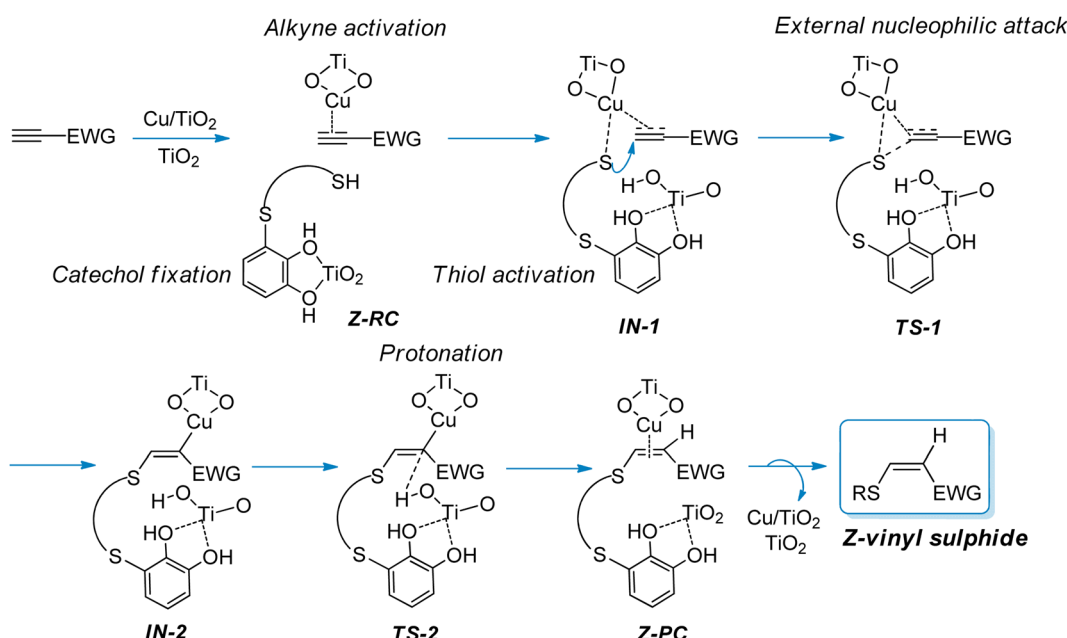


**Fig. 1** Possible interactions between thiol–catechol and  $\text{TiO}_2$  as catalyst support.

In fact, other materials tested as catalyst supports such as cellulose, zeolite-Y, activated carbon and MCM-41 gave no conversion into the desired vinyl sulphide products, while lower conversion values were observed when  $\text{ZnO}$ ,  $\text{Al}_2\text{O}_3$ ,  $\text{MgO}$  were used (72%, 68% and 47% respectively, Table S1†). In line with the results previously reported by Kodomari,<sup>18</sup> the use of  $\text{Al}_2\text{O}_3$  as the catalyst support resulted in a remarkable selectivity towards the *Z*-isomer (95 : 5, Table S1†).

In view of these observations, we proposed a plausible mechanistic pathway leading to the corresponding *Z*-vinyl sulphides, *via* a copper-catalysed *anti*-Markovnikov hydrothiolation process (Scheme 3), through an external nucleophilic attack from the thiol onto the carbon–carbon triple bond of the activated alkyne. Thus, we assume that both the alkyne and thiol are activated by copper, with the  $\text{TiO}_2$  support playing a non-innocent role in the catalytic process, probably through thiol S–H bond activation and by fixing the catechol moiety on the catalyst surface. As shown in Scheme 3, the protonated  $\text{TiO}_2$  would be responsible for the proton transfer step to give the final product and subsequent release of the catalyst to restart the catalytic cycle. In Scheme 3 the proposed structures for the reactive complex (RC), intermediates (IN), transition states (TS) and product complex (PC) are shown.

With the aim of better understanding the experimental results and also to find additional information on the reaction mechanism, we performed a computational study by using 3-((4-mercaptopbutyl)thio)benzene-1,2-diol and *propiolamide* as model starting materials. Since the reaction could be considered to start with the  $\text{CuNPs}/\text{TiO}_2$  nanocatalyst activating the alkyne and/or the thiol, it was necessary to establish the way in which the support surface could be attached to copper so as to stabilize the metal nanoparticles. Taking into account our



**Scheme 3** Proposed mechanistic pathway for the synthesis of *Z*-vinyl sulphides from activated alkynes and thiols bearing a catechol group catalysed by  $\text{CuNPs}/\text{TiO}_2$ .

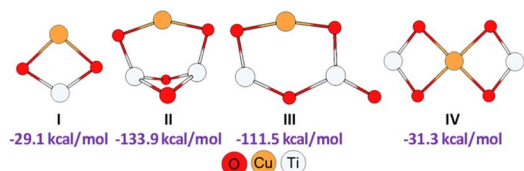


Fig. 2 Geometries and formation energies for the different  $\text{Cu}/(\text{TiO}_2)_n$  ( $n = 1, 2$ ) modelled structures (PBE0-D3BJ/Def2-TZVP/CPCM = DCM).

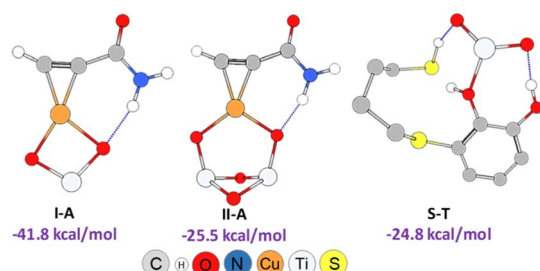


Fig. 3 Geometries and formation energies for the I-A, II-A and S-T structures (PBE0-D3BJ/Def2-TZVP/CPCM = DCM).

previous results on computational calculations for a similar copper nanocatalyst,<sup>25</sup> and assuming that copper would be attached to the support through both  $\text{TiO}_2$  oxygen atoms, we modelled different plausible structures for our  $\text{CuNPs}/\text{TiO}_2$  nanocatalyst. As can be seen from Fig. 2, this led us to propose

four stable structures, by including different  $\text{TiO}_2$  monomeric (**I**) and dimeric species (**II–IV**), being the planar monomeric structure **I** less exothermic than the dimeric ones.

Regarding the dimeric frameworks, planar structures **III** and **IV** were energetically less favourable than non-planar structure **II**, which resulted to be thermochemically more favoured, showing an exothermicity of  $-133.9 \text{ kcal mol}^{-1}$ .

As shown in Scheme 3, an external nucleophilic attack by a sulphur nucleophile onto the alkynyl copper complex, from the opposite side of the copper catalyst, would be the key step for the selective Z-vinyl sulphide formation. In order to facilitate the modelling of the stationary structures and to locate the transition states in a simpler way, we initially considered the formation of a reactive-like structure that we called reactive-complex (**RC**). In the **Z-RC** structure, the alkyne is being activated by copper, and the thiol-catechol is being fixed to the  $\text{TiO}_2$  support but is not yet coordinated with copper at this stage. For this purpose, we considered the formation of a  $\pi$ -complex between propiolamide and the structures **I** and **II** of the modelled nanocatalysts (Fig. 2), and we found that complex **I-A** was energetically more stable than structure **II-A** ( $-41.8$  and  $-25.5 \text{ kcal mol}^{-1}$  respectively, Fig. 3). Regarding the thiol-catechol, as discussed above, it would be fixed to the  $\text{TiO}_2$  support through coordination with the catechol hydroxyl groups, rendering the structure named **S-T** in Fig. 3, which was found to occur with an exothermicity of  $-24.8 \text{ kcal mol}^{-1}$ .

The **Z-RC** intermediate was then optimised ( $-110.3 \text{ kcal mol}^{-1}$ ) showing strong interactions between thiol-catechol and the  $\text{TiO}_2$  support, as set out in Fig. 1b. Specifically,

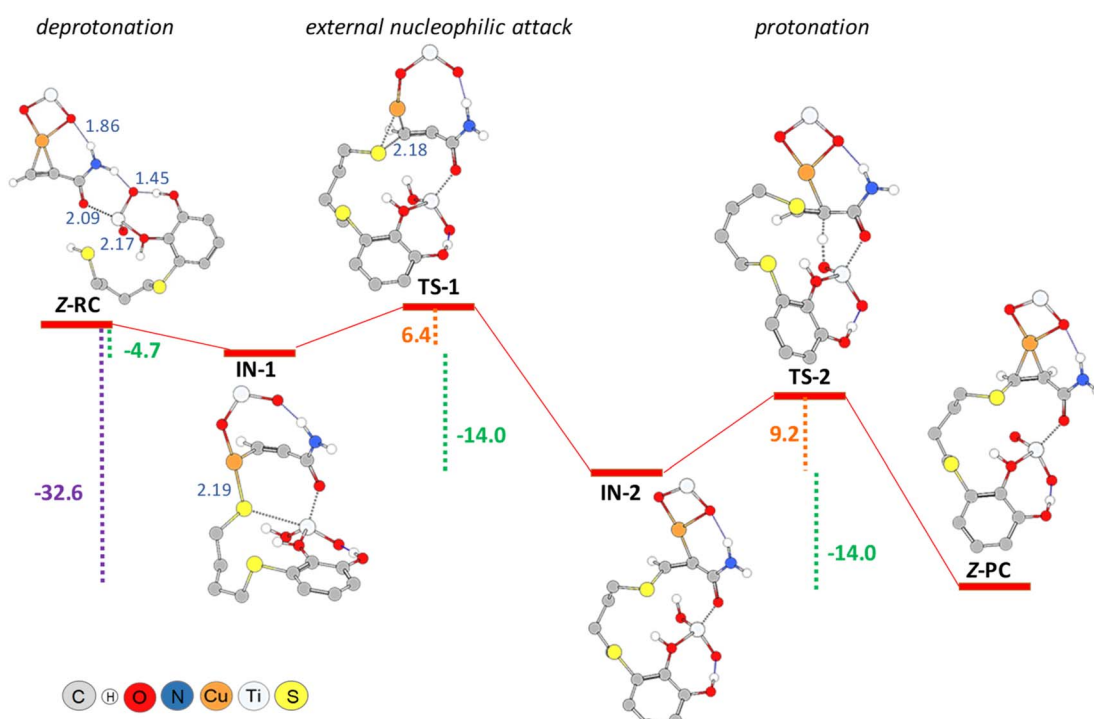


Fig. 4 PBE0-D3BJ/Def2-TZVP/CPCM = DCM potential energy profile ( $\text{kcal mol}^{-1}$ ) for thiol deprotonation, nucleophilic addition and protonation steps in the formation of Z-vinyl sulphide, showing interatomic distances ( $\text{\AA}$ , detailed in blue).



one of the O atoms of the catechol hydroxyl groups would be coordinating with a Ti atom in the support (2.17 Å), while the other hydroxyl group would be interacting through a hydrogen bond with one of the  $\text{TiO}_2$  oxygen atoms (1.45 Å). Stabilizing electrostatic interactions were also observed in all intermediates and transition states structures, both between the  $\text{H}_{\text{NH}_2}$  atom of propiolamide and one of the  $\text{TiO}_2$  oxygen atoms (**Z-RC**, 1.86 Å), and between a Ti atom and the  $\text{O}_{\text{C=O}}$  atom of the propiolamide (2.09 Å). By scanning the  $\text{S}_{\text{thiol}}\text{--C}_{\text{acetylenic}}$  reactive coordinate, starting from **Z-RC**, we found that thiol deprotonation (thiol activation) by Lewis basic sites of the support, would take place exothermically ( $-4.7 \text{ kcal mol}^{-1}$ ) without any activation barrier, to give the intermediate **IN-1** (Fig. 4), being this process also assisted by the formation of S–Cu bond (**IN-1**, 2.19 Å). All the mentioned interatomic distances are detailed in blue in Fig. 4.

In a subsequent step, through a nucleophilic addition, the S–C bond would be formed exothermically ( $-14.0 \text{ kcal mol}^{-1}$ ) with very low activation energy ( $6.4 \text{ kcal mol}^{-1}$ ), leading to the intermediate **IN-2** through a cyclic three-membered (S–Cu–C) transition state (**TS-1**). For the sake of comparison, the same reaction step was modelled by using another widely known

computational methodology for this kind of chemical reactive systems, such as the B3LYP functional<sup>33</sup> and 6-311+G\* basis set, and applying the same solvation model (CPCM = DCM). Thus, we found a relatively similar value for the activation energy ( $8.9 \text{ kcal mol}^{-1}$ ) but the process showed to be much less exothermic ( $-7.1 \text{ kcal mol}^{-1}$ ).

Turning again to the PBE0 functional method, we observed that the proton transfer step from  $\text{TiO}_2\text{-H}$  species to give the **Z-PC** intermediate was kinetically less favourable, and proceeded with an activation energy of  $9.2 \text{ kcal mol}^{-1}$ , thus being equally exothermic as the previous step ( $-14.0 \text{ kcal mol}^{-1}$ ). It is important to highlight that the full process, from **Z-RC** to **Z-PC**, was exothermic in  $32.6 \text{ kcal mol}^{-1}$ . Finally, both the active copper nanocatalyst and the support were regenerated, leading to the **Z-vinyl sulphide** product which showed a strong interaction between the O atom of the amide and one of the hydroxyl H atoms of catechol (**Z-VS**, 1.68 Å, Fig. 5).

On the other hand, taking into account that in the hydrothiolation of propiolamide the formation of minor amounts of the *E*-vinyl sulphide was experimentally observed during the hydrothiolation of propiolamide, we proposed that the formation of the *E*-isomer could proceed *via* the mechanism shown in Scheme 4. Since we considered that *E*-vinyl sulphide formation could proceed through an internal nucleophilic attack (from the same side of the copper catalyst) by a copper-coordinated sulphur nucleophile onto an alkynyl–copper complex, we employed the modelled structure **II** (Fig. 2) for the  $\text{Cu}/\text{TiO}_2$  nanocatalyst. In this case, as can be seen from **E-RC** structure, both the alkyne and thiol would be coordinated to copper, and the catechol hydroxyl groups would be fixed to the  $\text{TiO}_2$  support.

The DFT calculations showed that **E-RC** intermediate formation was much less exothermic ( $-57.1 \text{ kcal mol}^{-1}$ ) than **Z-RC**, with both O atoms of the catechol hydroxyl groups coordinated to a Ti atom of the support (2.25 and 2.29 Å), and the  $\text{S}_{\text{H}}$  atom coordinated with copper (2.35 Å), as represented in Fig. 1a

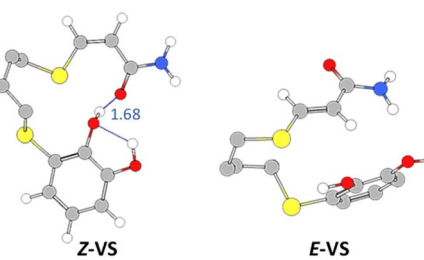
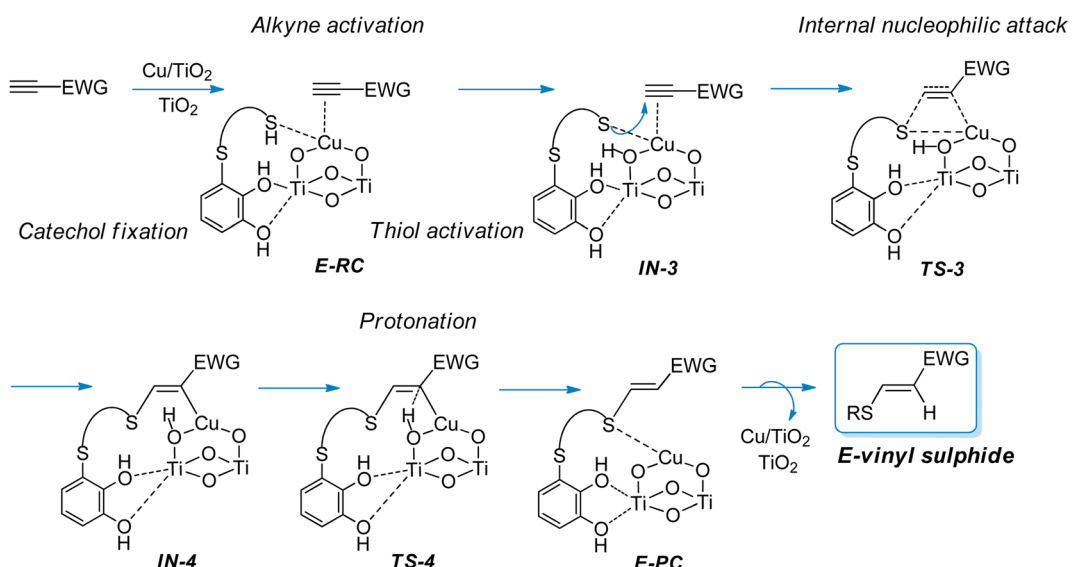


Fig. 5 Geometries and interatomic distances (Å, detailed in blue) for the vinyl sulphide isomers (PBE0-D3BJ/Def2-TZVP/CPCM = DCM).



Scheme 4 Proposed mechanistic pathway for the synthesis of *E*-vinyl sulphides from activated alkynes and thiols bearing a catechol group catalysed by  $\text{CuNPs}/\text{TiO}_2$ .

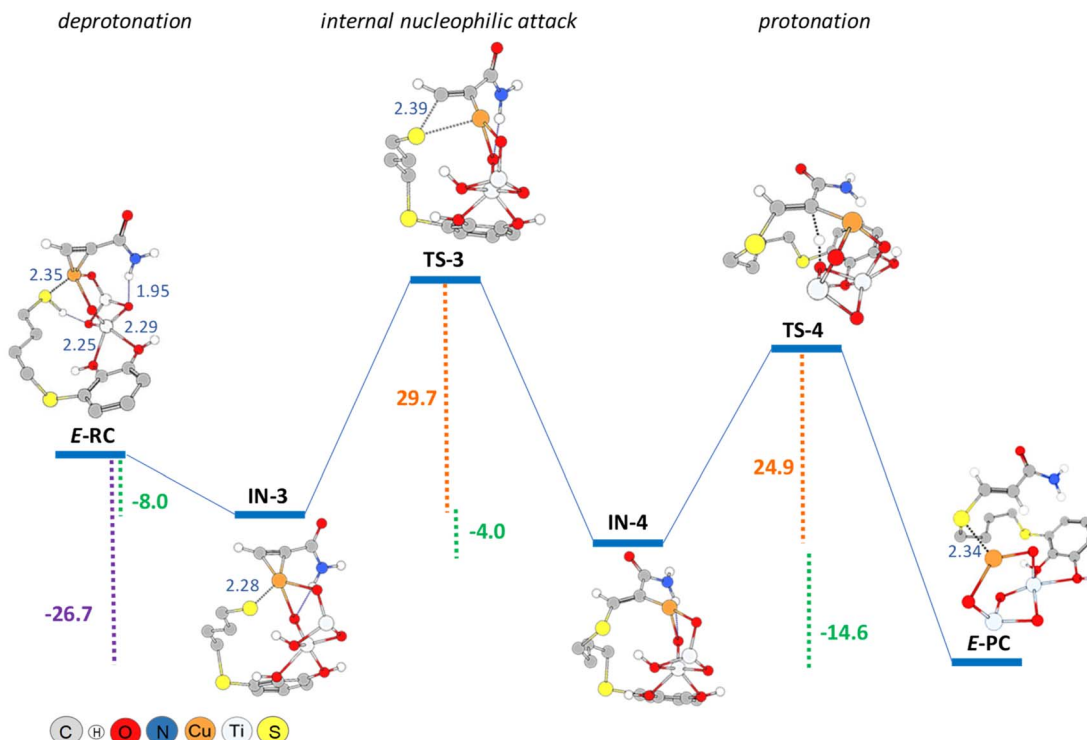


Fig. 6 PBE0-D3BJ/Def2-TZVP/CPCM = DCM potential energy profile ( $\text{kcal mol}^{-1}$ ) for thiol deprotonation, nucleophilic addition and protonation steps in the formation of *E*-vinyl sulphide, showing interatomic distances ( $\text{\AA}$ , detailed in blue).

and 6, respectively. As shown in Fig. 6, a stabilizing electrostatic interaction (**E-RC**, **IN-3**, **TS-3**, **IN-4**), between the  $\text{H}_\text{N}$  atom of propiolamide and one of the O atoms of the  $\text{TiO}_2$  support (**E-RC**,  $1.95 \text{\AA}$ ) was found.

As in the case of the *Z*-isomer, here again thiol deprotonation was shown to be exothermic ( $-8.0 \text{ kcal mol}^{-1}$ ) giving intermediate **IN-3** without any activation barrier, and through a pathway calculated to be  $3.3 \text{ kcal mol}^{-1}$  more exothermic than the deprotonation of the *Z*-isomer.

When modelling the nucleophilic addition step, we observed that formation of the S–C bond leading to the intermediate **IN-4**, occurred with an activation energy of  $29.7 \text{ kcal mol}^{-1}$ , that is more than  $20 \text{ kcal mol}^{-1}$  higher than that of the formation of **IN-2** (*Z*-isomer). As shown in Fig. 6, intermediate **IN-4** would be formed through a four-membered cyclic (C–S–Cu–C) transition state (**TS-3**), being also exothermic ( $-4.0 \text{ kcal mol}^{-1}$ ) but significantly less than that of the formation of **IN-2** ( $-14.0 \text{ kcal mol}^{-1}$ , *Z*-isomer). We consider that this could be probably due to the lack of coordination between titanium and the O atom of the amide group both in the corresponding intermediates and the transition states for the formation of the *E*-isomer. Another factor that could be energetically favouring the nucleophilic attack conducting to the *Z*-isomer, could be the distance between sulphur and carbon atoms in the corresponding transition states structures, which is  $2.18 \text{\AA}$  in **TS-1** (*Z*-isomer) and  $2.39 \text{\AA}$  in **TS-3** (*E*-isomer).

Here again, we also modelled this reaction step by employing B3LYP/6-311+G\* methodology. Thus, we found a very similar value for the activation energy to that observed when modelled

with PBE0 ( $29.2 \text{ kcal mol}^{-1}$ ) the process showing to be less exothermic ( $-1.8 \text{ kcal mol}^{-1}$ ).

As shown in Fig. 6, the last step involving the protonation from  $\text{TiO}_2$  support to give the **E-PC** intermediate, was observed to be kinetically similar (activation energy of  $24.9 \text{ kcal mol}^{-1}$ ) but much more exothermic ( $-14.6 \text{ kcal mol}^{-1}$ ) than the previous step. The observed activation barrier was notably higher than that of the same proton transfer step found for the formation of *Z*-isomer ( $24.9 \text{ vs. } 9.2 \text{ kcal mol}^{-1}$ ). In the **E-PC** modelled structure, copper from the nanocatalyst would be coordinated to sulphur atom at an interatomic distance of  $2.34 \text{\AA}$ , leading to the *E*-vinyl sulphide product that has no stabilizing interactions (Fig. 5).

It is important to note that the full process, from **E-RC** to **E-PC**, was exothermic in  $26.7 \text{ kcal mol}^{-1}$ , *i.e.*  $6 \text{ kcal mol}^{-1}$  less exothermic than that of the formation of the *Z*-isomer.

On the other hand, as previously reported by some of us,<sup>13</sup> when we carried out the hydrothiolation reaction between the thiol–catechol 1 and dimethyl acetylenedicarboxylate, catalysed by CuNPs/ $\text{TiO}_2$  under the same reaction conditions, a near 1 : 1 ratio (52 : 48) of the *Z*- and *E*-vinyl sulphide isomers were obtained. In order to explain this lack of selectivity, we computationally modelled the proposed mechanisms for the nucleophilic addition step leading to the formation of the corresponding *Z*- and *E*-vinyl sulphides (see ESI Fig. S1 and S2† for the complete mechanisms).

In agreement with the experimental results, as can be seen from Fig. 7, the activation barriers for the nucleophilic attack resulted energetically comparable,  $26.9 \text{ kcal mol}^{-1}$  (*Z*-isomer)



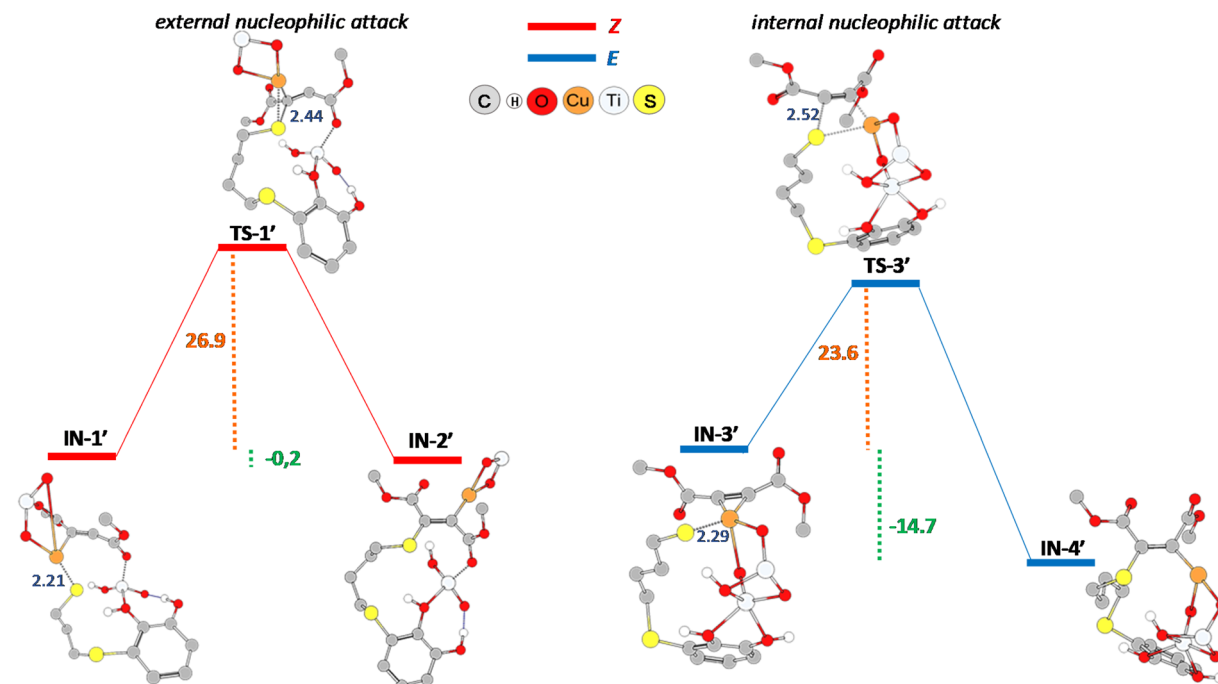


Fig. 7 PBE0-D3BJ/Def2-TZVP/CPCM = DCM potential energy profile ( $\text{kcal mol}^{-1}$ ) for the nucleophilic addition step in the formation of *Z*- (red line) and *E*-vinyl sulphide (blue line) derived from thiol-catechol **1** and dimethyl acetylenedicarboxylate. Interatomic distances ( $\text{\AA}$ ) are detailed in blue.

and  $23.6 \text{ kcal mol}^{-1}$  (*E*-isomer). In addition, transition state structures also show a similar sulphur–carbon distance, being  $2.44 \text{ \AA}$  (**TS-1'**) and  $2.52 \text{ \AA}$  (**TS-3'**), respectively. Although the mentioned reaction step is thermodynamically favoured for the formation of the *E*-isomer ( $-14.7 \text{ kcal mol}^{-1}$  vs.  $-0.2 \text{ kcal mol}^{-1}$ ), the subsequent protonation step is much more energetically demanding for this isomer ( $39.2 \text{ kcal mol}^{-1}$ , see Fig. S2,† formation of *E*-CP' structure) than the protonation step for the formation of *Z*-CP' structure ( $21.5 \text{ kcal mol}^{-1}$ , see Fig. S1†).

Finally, by comparing the nucleophilic addition steps leading to the formation of the corresponding *Z*-vinyl sulphides in the hydrothiolation of propiolamide (**IN-1** to **IN-2**, Fig. 4) and dimethyl acetylenedicarboxylate (**IN-1'** to **IN-2'**, Fig. 7), we found that the activation barrier for the former was notably lower ( $6.4 \text{ kcal mol}^{-1}$  for **TS-1** vs.  $26.9 \text{ kcal mol}^{-1}$  for **TS-1'**, see Fig. 4 and 7). This observation is in agreement with the shorter distance between sulphur and carbon atoms in **TS-1** transition state structure ( $2.18 \text{ \AA}$  for **TS-1** and  $2.44 \text{ \AA}$  for **TS-1'**). Moreover, even when this reaction step was exothermic for both starting alkynes, the formation of **IN-1** intermediate derived from propiolamide was exothermic by  $-14 \text{ kcal mol}^{-1}$  (Fig. 4), while the formation of **IN-1'** derived from dimethyl acetylenedicarboxylate was exothermic by only  $-0.2 \text{ kcal mol}^{-1}$  (Fig. 7). We think that this could be related, to a some extent, to the lack of extra stabilizing electrostatic interactions ( $\text{H}_{\text{NH}_2}-\text{O}_{\text{TiO}_2}$ ) as those observed for all the modelled structures in the formation of the *Z*-vinyl sulphide derived from the hydrothiolation of propiolamide.

## Conclusions

In sum, based on experimental results and DFT studies, we presented a detailed reaction mechanism for the  $\text{CuNPs/TiO}_2$ -catalysed hydrothiolation of activated alkynes with thiols bearing a catechol group, leading to the corresponding vinyl sulphides with high *Z*-stereoselectivity. We have suggested a plausible reaction mechanism that implies the activation of the carbon–carbon triple bond by coordination to a copper centre, followed by either an external or internal nucleophilic attack by the thiol-catechol, to give the corresponding *Z* or *E* isomer *via* a three membered cyclic  $\text{S}-\text{Cu}-\text{C}$  transition state or a four membered cyclic  $\text{C}-\text{S}-\text{Cu}-\text{C}$  transition state, respectively. It is important to mention that the computationally predicted selectivity for the reaction resulted higher than that observed experimentally, with both following the same trend. Besides, the proposed mechanism revealed the crucial synergistic role of the  $\text{TiO}_2$  support by: (i) fixing and activating the thiol-catechol, (ii) acting as a proton transfer agent in the deprotonation–protonation steps, and (iii) assisting in the control of stereoselectivity through a strong  $\text{Ti}-\text{O}_{\text{C}=\text{O}}$  coordination for the preferential formation of the *Z*-isomer.

Additionally, we proved that both functional PBE0 and B3LYP provided very similar and consistent energy profiles for the modelled reaction.

The mechanistic understanding of heterogeneous catalytic processes represents a big challenge and a need for both academic and industrial areas. As far as we know, this is the first computational mechanistic study about the alkyne hydrothiolation reaction by using thiol-catechols as functionalised

nucleophiles. We consider that the comprehensive mechanistic knowledge obtained from our work could be of relevance as a contribution for further rational design of new and efficient copper-based catalytic systems for the selective construction of S–Csp<sup>2</sup> bonds. The significance of the metal-catalysed hydrothiolation reaction in different fields, such as stereoselective organic synthesis, pharmaceuticals and functional materials, makes it essential to continue gaining better understanding of the mechanistic pathways involved, thus contributing to the rational development of improved catalytic systems.

## Author contributions

VD carried out the conceptualization, investigation, methodology and writing. FN participated in the investigation, methodology and writing. MC participated in the methodology. GR carried out the funding acquisition, the project administration, investigation and writing. All authors read and approved the final manuscript.

## Conflicts of interest

There are no conflicts to declare.

## Acknowledgements

This work was generously supported by the Consejo Nacional de Investigaciones Científicas y Técnicas (CONICET, PIP N°1665), Agencia Nacional de Promoción Científica y Tecnológica (ANPCyT, PICT-2018-2471) and Universidad Nacional del Sur (UNS, PGI 24/Q106) from Argentina. MC thanks the ANPCyT for a doctoral fellowship.

## Notes and references

- 1 K. Choudhuri, M. Pramanik, A. Mandal and P. Mal, *Asian J. Org. Chem.*, 2018, **7**, 1849–1855.
- 2 R. Castarlenas, A. Di Giuseppe, J. J. Pérez-Torrente and L. A. Oro, *Angew. Chem., Int. Ed.*, 2013, **52**, 211–222.
- 3 (a) M. Lo Conte, S. Pacifico, A. Chambery, A. Marra and A. Dondoni, *J. Org. Chem.*, 2010, **75**, 4644–4647; (b) L. Benati, L. Capella, P. C. Montevercchi and P. Spagnolo, *J. Chem. Soc., Perkin Trans. 1*, 1995, 1035–1038.
- 4 (a) S. Kanagasabapathy, A. Sudalai and B. C. Benicewicz, *Tetrahedron Lett.*, 2001, **42**, 3791–3794; (b) C. G. Screttas and M. Micha-Screttas, *J. Org. Chem.*, 1979, **44**, 713–719.
- 5 (a) A. Kondoh, K. Takami, H. Yorimitsu and K. Oshima, *J. Org. Chem.*, 2005, **70**, 6468–6473; (b) Z. L. Wang, R. Y. Tang, P. S. Luo, C. L. Deng, P. Zhong and J. H. Li, *Tetrahedron*, 2008, **64**, 10670–10675; (c) N. Zhao, C. Lin, L. Wen and Z. Li, *Tetrahedron*, 2019, **75**, 3432–3440.
- 6 (a) S. N. Riduan, J. Y. Ying and Y. Zhang, *Org. Lett.*, 2012, **14**, 1780–1783; (b) H. Ma, X. Ren, X. Zhou, C. Ma, Y. He and G. Huang, *Tetrahedron Lett.*, 2015, **56**, 6022–6029.
- 7 Y. Yang and R. M. Rioux, *Chem. Commun.*, 2011, **47**, 6557–6559.
- 8 A. Dondoni and A. Marra, *Eur. J. Org. Chem.*, 2014, 3955–3969.
- 9 (a) Z. Li, S. Zhao, Z. Wang, S. Zhang and J. Li, *J. Hazard. Mater.*, 2020, **396**, 122722; (b) K. Wei, B. Senturk, M. T. Matter, X. Wu, I. K. Herrmann, M. Rottmar and C. Toncelli, *ACS Appl. Mater. Interfaces*, 2019, **11**, 47707–47719.
- 10 (a) F. Nador, E. Guisasola, A. Baeza, M. A. Moreno-Villaécija, M. Vallet-Regí and D. Ruiz-Molina, *Chem.-Eur. J.*, 2016, **23**, 2753–2758; (b) J. Cui, Y. Yan, G. K. Such, K. Liang, C. J. Ochs, A. Postma and F. Caruso, *Biomacromolecules*, 2012, **13**, 2225–2228.
- 11 (a) M. A. Moreno-Villaécija, J. Sedó-Vegara, E. Guisasola, A. Baeza, M. V. Regí, F. Nador and D. Ruiz-Molina, *ACS Appl. Mater. Interfaces*, 2018, **10**, 7661–7669; (b) K. G. Malollari, P. Delparastan, C. Sobek, S. J. Vachhani, T. D. Fink, R. H. Zha and P. B. Messersmith, *ACS Appl. Mater. Interfaces*, 2019, **11**, 43599–43607.
- 12 (a) F. Nador, F. Novio and D. Ruiz-Molina, *Chem. Commun.*, 2014, **50**, 14570–14572; (b) F. Nador, K. Wnuk, J. García-Pardo, J. Lorenzo, R. Solorzano, D. Ruiz-Molina and F. Novio, *ChemNanoMat*, 2018, **4**, 183–193; (c) J. García-Pardo, F. Novio, F. Nador, I. Cavalieri, S. Suárez-García, S. Lope-Piedrafita, A. P. Candiota, J. Romero-Giménez, B. Rodríguez-Galván, J. Bové, M. Vila, J. Lorenzo and D. Ruiz-Molina, *ACS Nano*, 2021, **15**, 8592–8609.
- 13 F. Nador, J. Mancebo-Aracil, D. Zanotto, D. Ruiz-Molina and G. Radivoy, *RSC Adv.*, 2021, **11**, 2074–2082.
- 14 (a) J. Mancebo-Aracil, C. Casagualda, M. A. Moreno-Villaécija, F. Nador, J. García-Pardo, A. Franconetti-García, F. Busqué, R. Alibés, M. J. Esplandiu, D. Ruiz-Molina and J. Sedó-Vegara, *Chem.-Eur. J.*, 2019, **25**, 12367–12379; (b) J. Mancebo-Aracil, J. Sedó-Vegara and D. Ruiz-Molina, ICN2-CSIC, WO2019025498, 2019.
- 15 I. P. Beletskaya and V. P. Ananikov, *Chem. Rev.*, 2022, **122**, 16110–16293.
- 16 S. N. Riduan, J. Y. Ying and Y. Zhang, *Org. Lett.*, 2012, **14**, 1780–1783.
- 17 I. G. Trostyanskaya and I. P. Beletskaya, *Synlett*, 2012, **23**, 535–540.
- 18 M. Kodomari, G. Saitoh and S. Yoshitomi, *Bull. Chem. Soc. Jpn.*, 1991, **64**, 3485–3487.
- 19 J. Saiz-Poseu, J. Mancebo-Aracil, F. Nador, F. Busqué and D. Ruiz-Molina, *Angew. Chem., Int. Ed.*, 2019, **58**, 696–714 and references therein.
- 20 (a) U. Terranova and D. R. Bowler, *J. Phys. Chem.*, 2010, **114**, 6491–6495; (b) S. C. Li, J. G. Wang, P. Jacobson, X. Q. Gong, A. Selloni and U. Diebold, *J. Am. Chem. Soc.*, 2009, **131**, 980–984.
- 21 X. Zhang and K. Wang, *RSC Adv.*, 2015, **5**, 34439–34446.
- 22 L. T. Sahharova, E. G. Gordeev, D. B. Eremin and V. P. Ananikov, *ACS Catal.*, 2020, **10**, 9872–9888.
- 23 T. Vishwanath and K. Balakrishna, *J. Phys. Org. Chem.*, 2020, **33**, e4040.
- 24 (a) V. B. Dorn, M. A. Badajoz, M. T. Lockhart, A. B. Chopra and A. B. Pierini, *J. Organomet. Chem.*, 2008, **693**, 2458–2462; (b) M. E. Budén, V. B. Dorn, M. Gamba, A. B. Pierini and



R. A. Rossi, *J. Org. Chem.*, 2010, **75**, 2206–2218; (c) F. Nador, Y. Moglie, A. Ciolino, A. Pierini, V. Dorn, M. Yus, F. Alonso and G. Radivoy, *Tetrahedron Lett.*, 2012, **53**, 3156–3160; (d) V. B. Dorn, G. F. Silbestri, M. T. Lockhart, A. B. Chopra and A. B. Pierini, *New J. Chem.*, 2013, **37**, 1150–1156; (e) M. J. Lo Fiego, V. B. Dorn, M. A. Badajoz, M. T. Lockhart and A. B. Chopra, *RSC Adv.*, 2014, **4**, 49079–49085.

25 L. Fortunato, Y. Moglie, V. Dorn and G. Radivoy, *RSC Adv.*, 2017, **7**, 18707–18713.

26 (a) F. Neese, *Wiley Interdiscip. Rev.: Comput. Mol. Sci.*, 2012, **2**, 73–78; (b) F. Neese, *Wiley Interdiscip. Rev.: Comput. Mol. Sci.*, 2017, **8**, e1327.

27 W. Kohn and J. J. Sham, *Phys. Rev.*, 1965, **140**, A1133–A1138.

28 C. Adamo and V. Barone, *J. Chem. Phys.*, 1999, **110**, 6158–6169.

29 (a) S. Grimme, S. Ehrlich and L. Goerigk, *J. Comput. Chem.*, 2011, **32**, 1456–1465; (b) S. Grimme, J. Antony, S. Ehrlich and H. Krieg, *J. Chem. Phys.*, 2010, **132**, 154104.

30 B. Dereli, M. A. Ortúñoz and C. J. Cramer, *ChemPhysChem*, 2018, **19**, 959–966.

31 F. Weigend and R. Ahlrichs, *Phys. Chem.*, 2005, **7**, 3297–3305.

32 V. Barone and M. J. Cossi, *Phys. Chem.*, 1998, **102**, 1995–2001.

33 (a) C. Lee, W. Yang and R. G. Parr, *Phys. Rev. B: Condens. Matter Mater. Phys.*, 1988, **37**, 785–789; (b) A. D. Becke, *Phys. Rev. A*, 1988, **38**, 3098–3100; (c) E. Miehlich, A. Savin, H. Stoll and H. Preuss, *Chem. Phys. Lett.*, 1989, **157**, 200–206.

